AD-A046 118 NAVAL OCEAN SYSTEMS CENTER SAN DIEGO CALIF F/G 4/1
AEROSOL EXTINCTION OF PHOTOPIC AND IR WAVELENGTHS. DEMONSTRATED--ETC(U)
AUG 77 H G HUGHES

UNCLASSIFIED NOSC/TR-143 NL

1 OF 1
ADA
046118

END
DATE
FILMED
12-77
DDC

NOSC

NOSC / TR 143

AD A046118

Technical Report 143

AEROSOL EXTINCTION OF PHOTOPIC AND IR WAVELENGTHS

Demonstrated relationship of visibility to atmospheric liquid water suggests that atmospheric transmittance for IR can be estimated by use of simple measurements and scaling laws

HG Hughes

23 Aug 1977

Prepared for
Naval Air Systems Command

Final report, for period October 1976 through June 1977

F52521

F52521

Approved for public release; distribution is unlimited

NAVAL OCEAN SYSTEMS CENTER
SAN DIEGO, CALIFORNIA 92152

393 159

NAVAL OCEAN SYSTEMS CENTER, SAN DIEGO, CA 92152

AN ACTIVITY OF THE NAVAL MATERIAL COMMAND

RR GAVAZZI, CAPT, USN
Commander

HOWARD L BLOOD, PhD
Technical Director

ADMINISTRATIVE INFORMATION

Work was conducted under project number F525 for the Naval Environmental Prediction Research Facility under the auspices of Naval Air Systems Command, Code 370C and NOSC IR/IED work unit Z117 by the Electromagnetic Propagation Division. The report covers the period October 1976 through June 1977 and was approved for publication 23 August 1977.

The author expresses thanks to Dr DR Jensen, who provided the aerosol-size distribution measurements, and to Mr J Woodward, who assisted in the data reduction.

Released by
JH Richter, Head
EM Propagation Division

Under authority of
JD Hightower, Head
Environmental Sciences Department

UNCLASSIFIED

SECURITY CLASSIFICATION OF THIS PAGE (When Data Entered)

REPORT DOCUMENTATION PAGE		READ INSTRUCTIONS BEFORE COMPLETING FORM
1. REPORT NUMBER NOSC Technical Report 143 (TR 143)	2. GOVT ACCESSION NO.	3. RECIPIENT'S CATALOG NUMBER
4. TITLE (and Subtitle) AEROSOL EXTINCTION OF PHOTOPIC AND IR WAVELENGTHS (Demonstrated relationship of visibility to atmospheric liquid water suggests that atmospheric transmittance for IR can be estimated by use of simple measurements and scaling laws)		5. TYPE OF REPORT & PERIOD COVERED Final, October 1976 through June 1977 6. PERFORMING ORG. REPORT NUMBER
7. AUTHOR(s) HG Hughes		8. CONTRACT OR GRANT NUMBER(s)
9. PERFORMING ORGANIZATION NAME AND ADDRESS Naval Ocean Systems Center San Diego, CA 92152		10. PROGRAM ELEMENT, PROJECT, TASK AREA & WORK UNIT NUMBERS F525 and Z117
11. CONTROLLING OFFICE NAME AND ADDRESS Naval Air Systems Command (Code 370C)		12. REPORT DATE 23 August 1977 13. NUMBER OF PAGES 14
14. MONITORING AGENCY NAME & ADDRESS (if different from Controlling Office)		15. SECURITY CLASS. (of this report) Unclassified 15a. DECLASSIFICATION/DOWNGRADING SCHEDULE

16. DISTRIBUTION STATEMENT (of this Report)

Approved for public release; distribution is unlimited

17. DISTRIBUTION STATEMENT (of the abstract entered in Block 20, if different from Report)

18. SUPPLEMENTARY NOTES

19. KEY WORDS (Continue on reverse side if necessary and identify by block number)

Aerosols

Atmospheric attenuation

Optical communication

20. ABSTRACT (Continue on reverse side if necessary and identify by block number)

Marine aerosol-size distributions are measured and scaling laws derived to relate the photopic and infrared extinction coefficients for differing visibility conditions. It is shown that simple linear relationships can be derived for this purpose by use of the measured distributions and Mie theory. Linear relationships can also be derived to relate wavelength-dependent extinctions to atmospheric liquid water content. Comparison of extinctions predicted analytically on the basis of accepted fog aerosol models and those numerically derived from measured distributions indicates that the contributions from particles having diameters greater than 30 micrometres may significantly alter the derived scaling laws.

DD FORM 1 JAN 73 1473 EDITION OF 1 NOV 65 IS OBSOLETE S/N 0102-014-6601

UNCLASSIFIED

SECURITY CLASSIFICATION OF THIS PAGE (When Data Entered)

OBJECTIVE

Determine the feasibility of scaling photopic atmospheric transmission to the infrared wavelengths for a marine environment. Specifically, conduct measurements of marine aerosol-size distributions and, by using Mie theory, derive scaling laws to relate the photopic and infrared extinction coefficients for differing visibility conditions.

RESULTS

1. Simple linear relationships can be derived, by using Mie theory and measured aerosol-size distributions, which relate the photopic and infrared atmospheric extinction coefficients.

2. Similarly, linear relationships can be derived which relate the wavelength-dependent extinctions to the atmospheric liquid water content.

3. Different linear relationships for each wavelength are derived depending upon whether the meteorological visibility is less than or greater than about 4 kilometres.

4. Measured meteorological visibilities are closely related to measured atmospheric liquid water contents. This suggests that simple visiometer or laser backscatter (lidar) measurements can be used with scaling laws to estimate atmospheric transmittance for infrared wavelengths.

5. Comparison of extinctions predicted analytically on the basis of accepted fog aerosol models and those numerically derived from measured distributions indicates that the contributions from particles having diameters greater than 30 μm may significantly alter the derived scaling laws.

RECOMMENDATIONS

1. Continue measurements of aerosol-size distributions in a variety of marine environments. Extend the measurement capabilities of the Knollenberg spectrometer to include those particles having diameters exceeding 30 μm.

2. Obtain airborne measurements of aerosol-size distributions such that scaling laws can be obtained which include horizontal and vertical variations in aerosol concentrations.

3. Extend the instrumentation capabilities to include both pulsed and FM-cw lidars to remotely sense extinction coefficients and water contents.

CONTENTS

ILLUSTRATIONS

INTRODUCTION

The performance of existing and planned Navy shipboard electro-optical (EO) systems which utilize infrared (IR) wavelengths is severely limited by the constituents of the atmosphere and the inhomogeneities in their concentrations. The ability of an EO system to perform a function—ie, detect or identify a target within specified probability limits—depends upon the target irradiance signal-to-noise (background plus internal) ratio. The irradiance signal-to-noise ratio is degraded by atmospheric extinction, which is the sum of absorption and scattering by aerosols and molecular gases. The contributions to the extinction from molecular water vapor are important at IR wavelengths and can usually be assessed by standard meteorological measurements. More difficult to assess are the contributions from aerosols and changes in their size distributions, which depend to a large extent upon relative humidity changes. In situ measurements of aerosol-size distributions made with groundbased or airborne devices (Knollenberg spectrometers, impactors, etc), together with Mie theory, provide a way for estimating atmospheric aerosol extinction at different wavelengths. These devices are usually expensive and impractical for operational fleet uses. Needed to assist system planners and users in predicting the performance of shipboard EO systems are (1) remote sensing techniques for relating meteorological parameters (which are unaffected by the local shipboard environment) to the extinction at visible wavelengths, and (2) scaling laws which then relate the visible extinction to that in the IR band.

Bieberman et al (1977) recently published results based on continental aerosol-size distribution measurements at Grafenwöhr, Federal Republic of Germany, during the 1975–76 winter, relating the liquid water content to the aerosol extinction coefficient. They suggest that a scaling of the photopic transmission to the IR wavelengths is possible and that the scaling laws are independent of the particle-size distributions. From the earlier work of Houghton (1939) and others as referenced by Eldridge (1966), it is recognized that a general inverse relationship exists between the atmospheric liquid water content and the visibility as defined by Koschmieder's formula ($V_m = 3.92/\beta_{ae}$ where β_{ae} is the aerosol extinction coefficient). However, the relation between the visibility or extinction coefficient and the liquid water content is inherently dependent upon the aerosol-size spectrum for clear weather conditions. Only for the poorer visibility conditions, such as fog, is the relationship determined primarily by the largest droplets present and not so much the individual distribution.

In this report, aerosol-size distributions measured prior to and during a coastal marine fog are presented. Together with Mie theory, the measured distributions are used to derive scaling laws which relate the liquid water content to the photopic and IR extinction coefficients for the differing visibility conditions.

MEASUREMENTS

In addition to the standard surface meteorological observations, aerosol-size distributions are routinely made at the NOSC remote sensing facility located on the sea side of Point Loma in San Diego, California. The frequently occurring coastal marine fogs related to Santa Ana or stratus lowering events provide the opportunity to make atmospheric measurements

---

Biberman, LM, Roberts, RE, and Seekamp, LN, A comparison of electro-optical technologies for target acquisition and guidance, Institute for Defense Analysis, paper P-1218, January 1977

Houghton, HG, On the relationship between visibility and the constitution of clouds and fog, Jour Aero Sci, 6, 408, 1939

Eldridge, RG, Haze and fog aerosol distributions, Jour Atmos Sci, 23, 605, 1966

in a variety of reduced visibility conditions. For this analysis aerosol-size distributions are used which were obtained during a 10-hour period on 15 February 1977 when the visibility varied from approximately 0.1 to 6 km. The distributions were measured by using an aspirated Knollenberg ASSP-100 spectrometer probe mounted atop a building approximately 45 metres above mean sea level. The spectrometer sizes particles in four overlapping bands which are individually divided into 15 different diameter intervals. Spectra are measured in each range-band every second and digitally recorded on magnetic tape. The digitized data are subsequently processed on a Data General Corporation NOVA 800 computer. Individual spectra in each range-band were averaged for 4 minutes, and then combined to give a diameter coverage from 0.45 to 29.4 μm. The liquid water density was also computed by integrating the averaged size distributions assuming the aerosols to be predominately spherical water droplets. Throughout the 10-hour period the meteorological visibility was measured with a forward scatter fog visiometer (Meteorology Research Inc model 1580) which was located adjacent to the Knollenberg spectrometer. Figure 1 shows the liquid water density computed from the measured size distributions at 5-minute intervals for the 10-hour period and the measured meteorological visibility. Good inverse correlation is evident between the liquid water content and the visibility for the entire period.

Examples of the measured size distributions are shown in figure 2. Prior to (0215Z and 0245Z) and after (0300Z and 0315Z) the advection of the fog over the recording station the distributions approximate inverse power laws for diameters greater than 1–2 μm with diameter exponents of 3.95, 3.55, 2.53, and 2.73, respectively. The number densities at diameters greater than 5 μm increased two orders of magnitude during the fog.

DATA ANALYSIS

A computer program (compiled by Stone, 1976) was used to calculate the extinction, scattering, and absorption coefficients for optical propagation through aerosols and at wavelengths of 0.53, 1.06, 3.5, and 10.6 μm. The contributions to absorption by molecular gases have not been included in the calculations. Basically, the program evaluates the integral

$$\beta_{\substack{ae \\ as}} = \int_{r_o}^{r_1} \pi r^2 \, n(r) \, K_{\substack{e \\ s}} (r/\lambda, \eta) \, dr \quad , \tag{1}$$

where the coefficients of concern are designated by β and the subscripts ae and as refer to aerosol extinction and scattering, respectively. The aerosol absorption coefficient is then determined by

$$\beta_{aa} = \beta_{ae} - \beta_{as} \quad . \tag{2}$$

In equation (1), n(r) is the number of particles per unit volume having radii between r and r + dr. $K_{\substack{e \\ s}}(r/\lambda, \eta)$ is the total cross section for extinction or scattering determined by Mie theory and normalized to the spherical particle geometrical cross section. η is the complex index of refraction of liquid water at a wavelength λ as presented by Deirmendjian (1964).

Stone, WR, MIE and SCATCO: Programs to compute the scattering, extinction, and absorption properties of optical propagation through particle distributions, MEGATEK Corporation, San Diego, CA, Report R2005-070-F-1, 1 November 1976

Deirmendjian, D, Scattering and Polarization Properties of Water Clouds and Hazes in the Visible and Infrared, Applied Optics, 3(2), 187, 1964

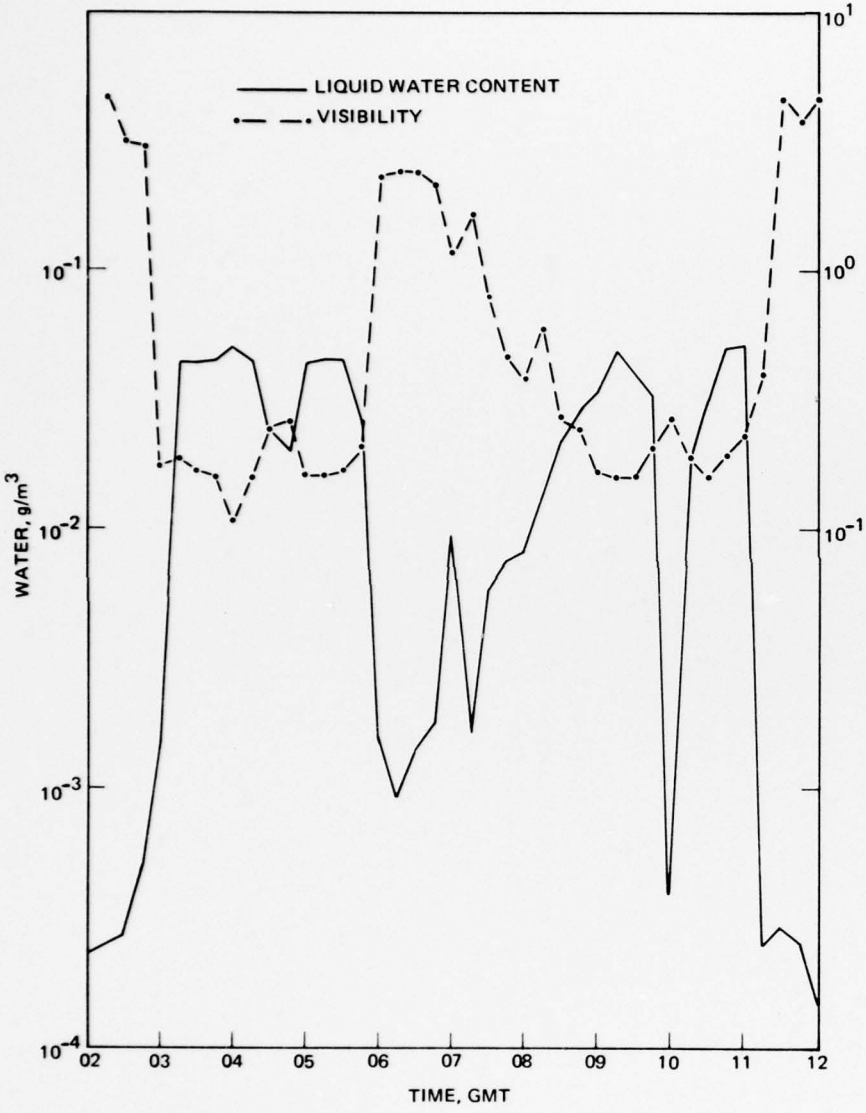

Figure 1. Total liquid water content (determined from integrated drop-size distributions compared with the meteorological visibility (measured with a forward scatter visiometer) as a function of time.

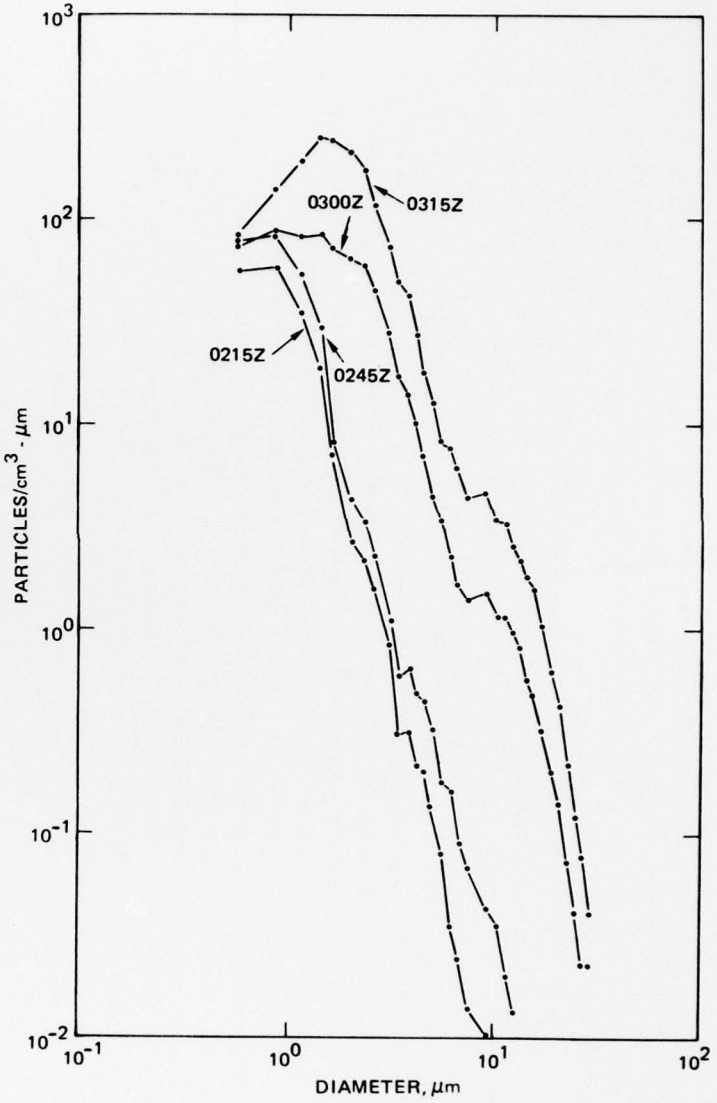

Figure 2. Examples of drop-size distributions measured before (0215Z and 0245Z) and after (0300Z and 0315Z) the onset of fog on 15 February 1977.

Actually, equation (1) is integrated by using Simpson's rule over unequally spaced intervals. In the integration a third-order polynomial fit is used to interpolate the measured distributions between the diameter interval midpoints to fit the size parameters for which the Mie coefficients are given.

Figure 3 shows the extinction coefficients calculated at 10-minute intervals for the initial 4-hour period. The extinction coefficients closely follow the liquid water density variations, as is to be expected, since both are determined by integrating the size distributions. Of significance are the different relations between the visible (0.53 μm) extinction and the extinctions for the IR wavelengths before and after the onset of fog. Before the fog the 0.53-μm wavelength suffers the greatest extinction, while after the fog onset there is little difference between the extinctions of the three smaller wavelengths. The ratio of the 0.53- and 10.6-μm extinctions changes by approximately a factor of 5 after the onset of fog. These differences illustrate the visibility dependence on any scaling laws one would derive from the measured size distributions. This is further evidenced in figure 4, where the ratios of the scattering to absorption coefficients at 3.5 and 10.6 μm are shown as a function of time. Before and after the fog onset the extinction at 3.5 μm is primarily absorption while at 10.6 μm absorption dominates before the fog and scattering dominates after the fog onset. However, these results may be significantly altered, particularly for the 10.6-μm wavelength, when contributions to the size distributions from droplets with diameters greater than 30 μm are included in the calculations.

In figure 5 the aerosol extinction coefficients at 3.5 and 10.6 μm are plotted versus those at 0.53 μm. The 1.06-μm extinctions are excluded because they differ only slightly from those for 0.53 μm. Regression analyses of the data show different linear relationships between the photopic and IR extinctions for visibilities less than and greater than 4 km. Similarly in figure 6, different linear relationships are derived between the liquid water density and the 0.53-μm extinction for water densities less than and greater than 0.005 g/m^3. Although the correlation coefficients (r) for the different regressions are good, there is considerable scatter in the data before the fog, especially for the 10.6-μm wavelength, which again illustrates the dependency on the individual distributions. This dependency can be removed, somewhat, if the data in figures 5 and 6 are normalized to the total number of particles per unit volume, N, in each distribution, as shown in figures 7 and 8, respectively. However, to be of practical value, any scaling laws derived from the figures would require as inputs the individual size distributions as well as the liquid water content.

From the regression analyses in figures 5 and 6, the following equations can be derived which relate the aerosol extinction at each wavelength to the liquid water contents $W_1 > 0.005$ g/m$^3 > W_2$:

$$\beta_{ae}(1.06\ \mu\text{m}) = \begin{cases} 74\, W_1^{0.72} \\ 622\, W_2^{1.1} \end{cases} \tag{3a}$$

$$\beta_{ae}(3.5\ \mu\text{m}) = \begin{cases} 184\, W_1^{0.99} \\ 15\, W_2^{0.69} \end{cases} \tag{3b}$$

$$\beta_{ae}(10.6\ \mu\text{m}) = \begin{cases} 264\, W_1^{1.4} \\ 27\, W_2^{0.96} \end{cases} \tag{3c}$$

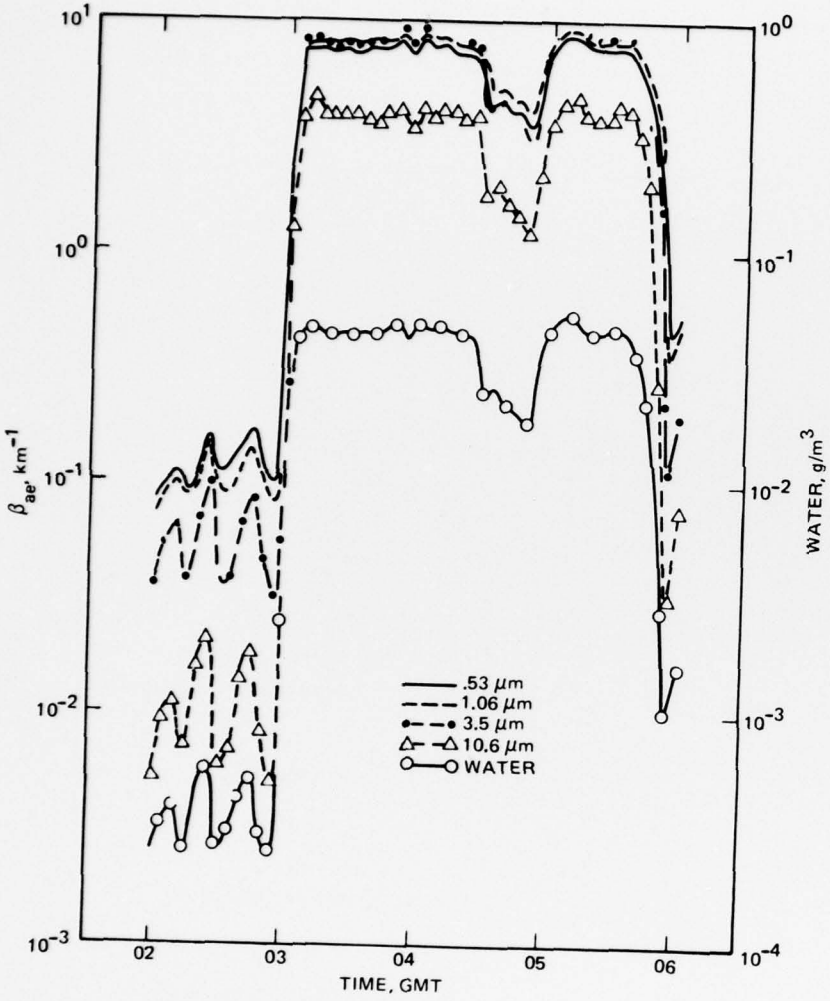

Figure 3. Aerosol extinction coefficient and liquid water content as a function of time.

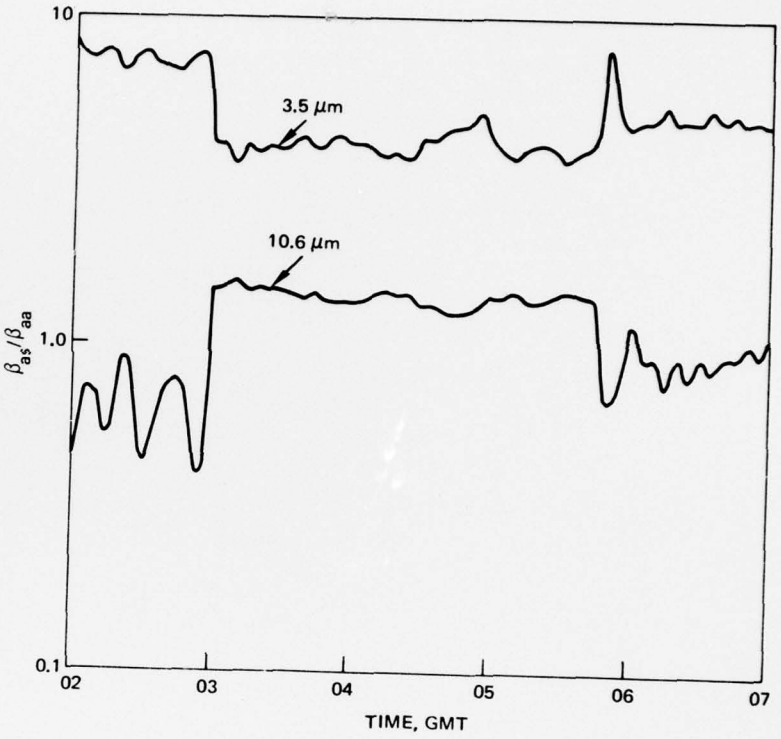

Figure 4. Ratio of scattering to absorption coefficient for 3.5 and 10.6 μm as a function of time.

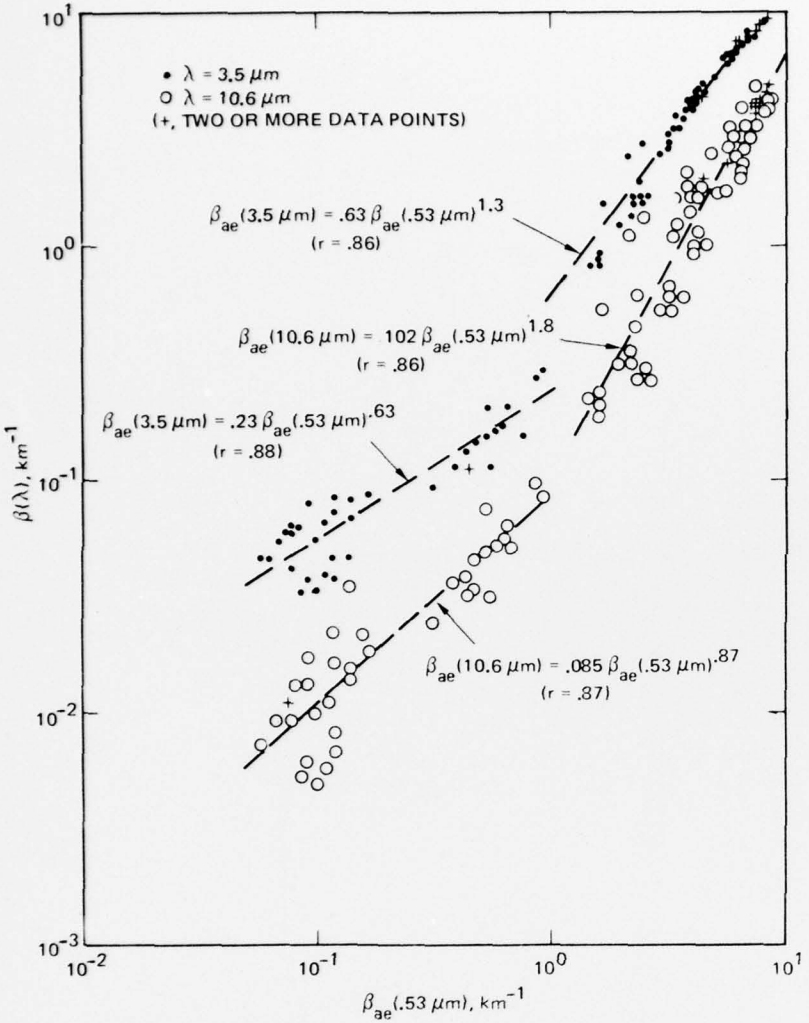

Figure 5. Aerosol extinction coefficients at 3.5 and 10.6 μm vs that at 0.53 μm. The regression analyses indicate the differing relationships between extinctions before and after the onset of the fog period on 15 February 1977.

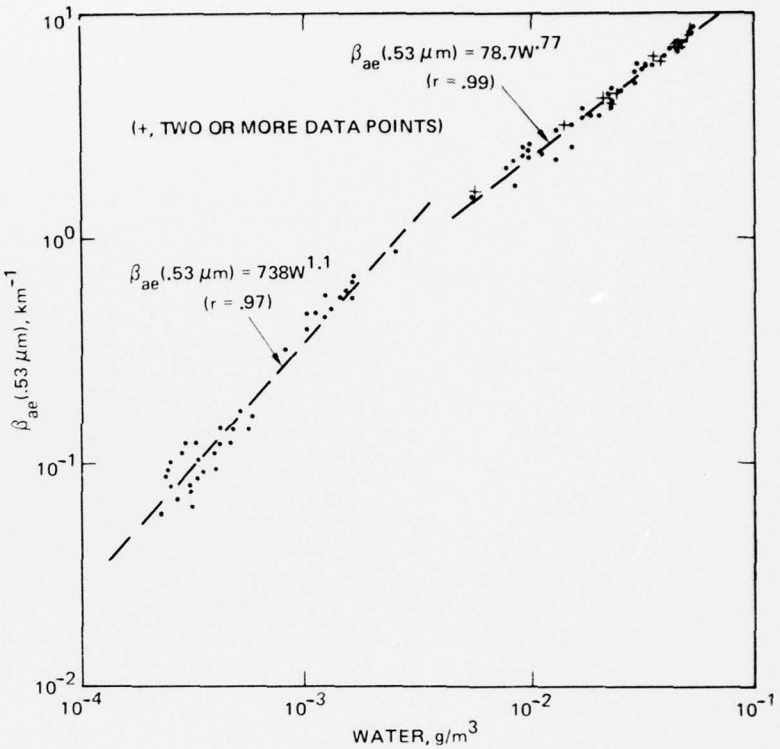

Figure 6. Calculated extinction coefficient of 0.53 μm vs liquid water content. The regression analyses indicate the differing relationships between extinction and water content before and after the onset of the fog period on 15 February 1977.

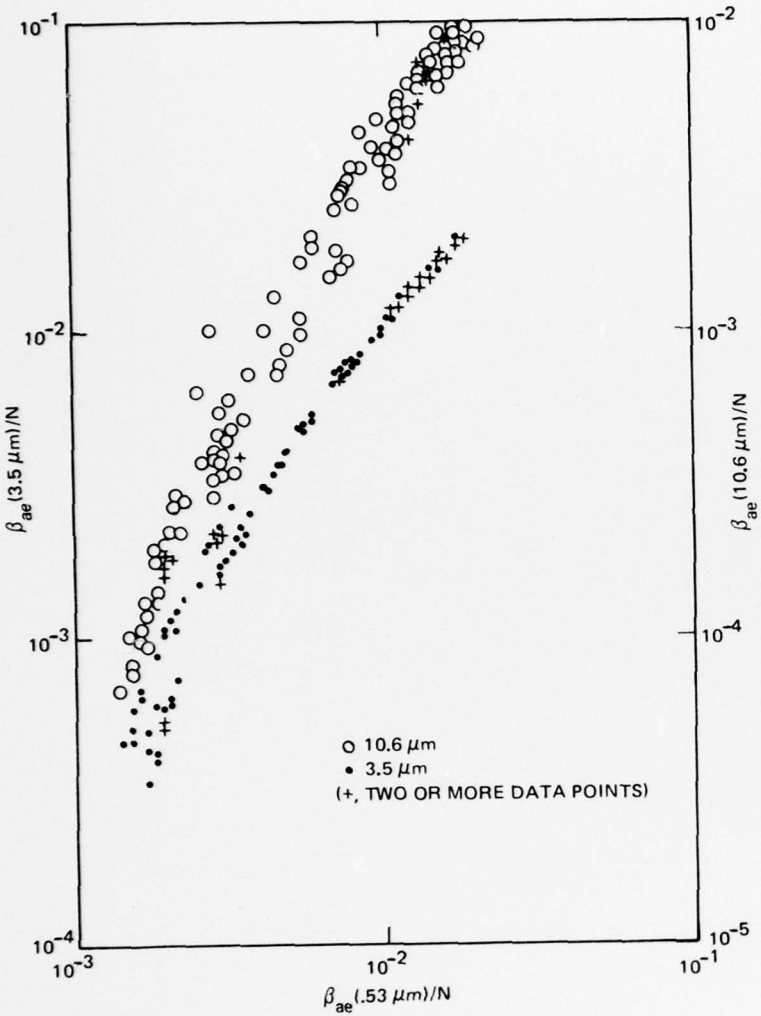

Figure 7. Calculated extinction coefficients at 3.5 and 10.6 μm vs that at 0.53 μm and normalized to the total particle number density.

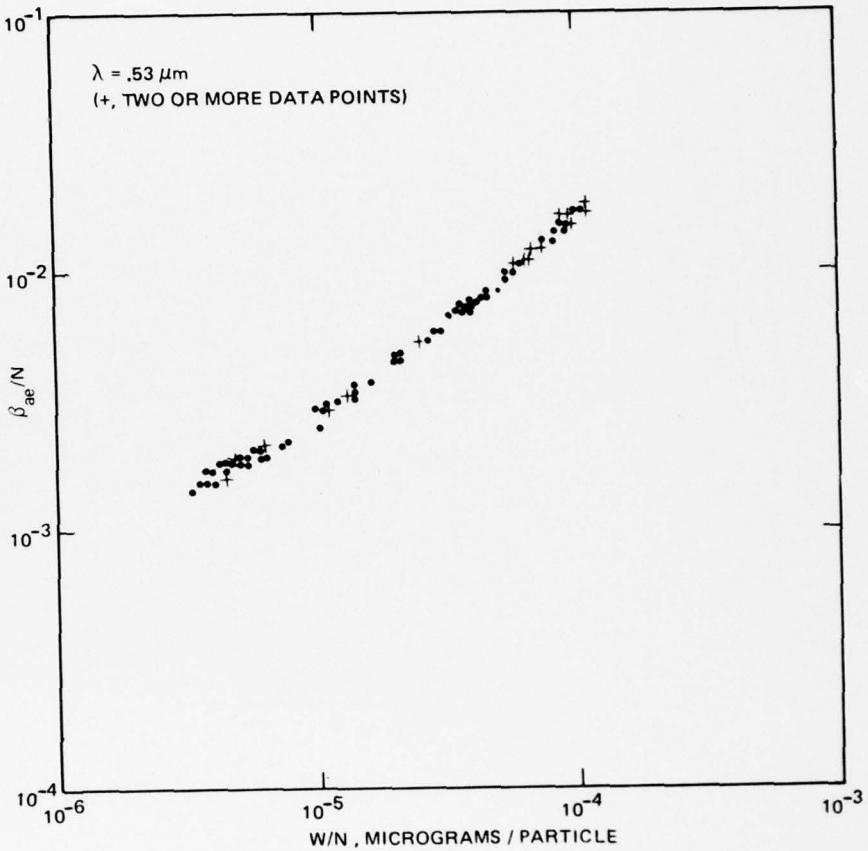

Figure 8. Calculated extinction coefficient at 0.53 μm vs the liquid water content and normalized to the total particle number density.

In figure 9, the extinctions derived for different water densities by using the 15 February scaling laws are compared with those calculated from selected individual size distributions measured during different fog periods which occurred 8 and 17 February 1977. The good agreement indicates a consistency in the size distributions for the different fog periods and demonstrates the utility of the scaling laws. It is evident that IR extinction coefficients can be estimated from simple scaling laws using visiometer measurements of the photopic extinction or remote sensing techniques such as laser ranging devices (lidar), as suggested by Roberts (1976), whose backscatter profile is sensitive to the liquid water content along the propagation path.

COMPARISON WITH THEORY

There is little difference between the 0.53- and 3.5-μm extinctions shown in figure 9 for water contents greater than about 0.03 g/m^3. The falloff in the curves at 10.6 μm may simply be caused by limiting the maximum radius to 14.2 μm (the midpoint of the highest range-band of the Knollenberg spectrometer). Had larger drop sizes been measurable by the Knollenberg probe, their contribution to the 10.6-μm extinctions, due to increased absorption, might have flattened the curves over the wavelength band considered for the higher water densities. However, the near flatness of curves between 0.53 and 3.5 μm allows an analytical expression for extinction to be obtained which is primarily dependent on the liquid water density and not so much on the individual size distributions for heavy fogs.

On the basis of experimental results obtained worldwide, Junge (1952) concluded the size distributions of "large and giant" particles could be approximated by the simple law

$$n(r) = C\, r^{-p} \quad , \tag{4}$$

where C and p are constants. Equation (1) can now be written

$$\beta_{ae} = C\pi \int_{r_o}^{r_1} r^{2-P}\, K(r/\lambda)\, dr \quad . \tag{5}$$

Changing the variable of integration to $a = r_1/\lambda$ one obtains

$$\beta_{ae} = C\pi\lambda^{3-p} \int_{o}^{r_1} a^{2-p}\, K(a)\, da \quad , \tag{6}$$

where the lower limit of integration is ignored because $r_o \ll r_1$. Now $\beta = f(\lambda, a)$ and $a = f(r_1, \lambda)$ such that the total differential of β is defined by

$$d\beta = \frac{\partial\beta}{\partial\lambda}\, d\lambda + \frac{\partial\beta}{\partial a} \cdot \frac{\partial a}{\partial\lambda} \cdot d\lambda \quad . \tag{7}$$

Roberts, RE, Atmospheric transmission modeling: Proposed aerosol methodology with application to the Grafenwöhr atmospheric optics data base, Institute for Defense Analysis, paper P-1225, December 1976

Junge, C, The size distribution and aging of natural aerosols as determined from electrical and optical data of the atmosphere, Jour Meteor, 12, 13, 1955

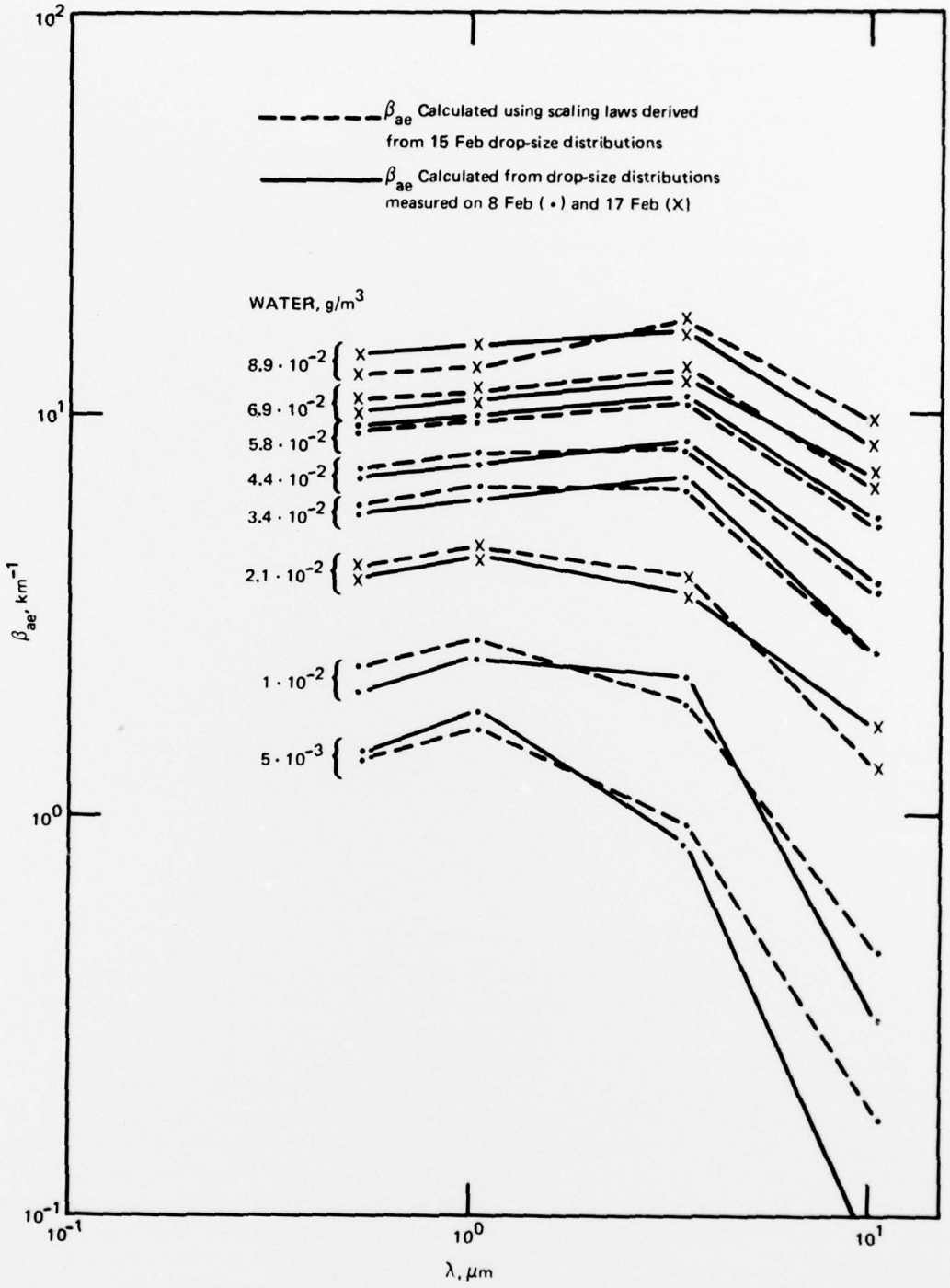

Figure 9. Aerosol extinction coefficients calculated by using scaling laws derived from 15 February distributions compared with those determined from individual distributions measured during fog periods on 8 February and 17 February 1977.

Performing the required operations on (6) and substituting into (7), Kurnick et al (1960) arrived at the following expression (which is similar to one derived by Junge):

$$\frac{d(\ell n\, \beta_{ae})}{d(\ell n\, \lambda)} = (3 - p) - \frac{C\pi\, r_1^{3-p}}{\beta_{ae}}\, K(r_1/\lambda) \quad . \tag{8}$$

By using (4), the constant C in (8) can be determined from the liquid water density given by

$$W = C \int_{r_o}^{r_1} 4/3\, \pi\, r^{3-p}\, \rho\, dr \quad , \tag{9}$$

where ρ is the water density. For $p < 4$, and ignoring the lower limit, integration of (9) yields

$$W \simeq \frac{0.75\pi\, C\, r_1^{4-p}}{(4-p)\,\rho} \quad , \tag{10}$$

from which C can be obtained, and (8) then becomes

$$\frac{d(\ell n\, \beta_{ae})}{d(\ell n\, \lambda)} = (3 - p) - \frac{.75(4-p)\, K(r_1/\lambda)\, W}{r_1\, \rho\, \beta_{ae}} \quad . \tag{11}$$

Junge (1952) deduced that $p \to 2$ for fogs. Also, when $r_1/\lambda \gg 1$, $K(r_1/\lambda) \to 2$. Figure 8 shows that $d(\ell n\, \beta_{ae})/d(\ell n\, \lambda) \simeq 0$ for the higher water densities such that (11) can be solved for the extinction coefficient to give

$$\beta_{ae} \simeq 211\, W, \text{ km}^{-1} \tag{12}$$

where r_1 was taken as 14.2 μm and W has units of g/m^3.

In figure 10 the extinctions derived by using the Junge fog model are compared with the regression analyses (equation (3)) for the higher water densities. For the measured size distributions the condition that $r_1/\lambda \gg 1$ is satisfied only for the 0.53- and 1.06-μm wavelengths. The close agreement between the 3.5-μm regressions and the analytical values is probably fortuitous since $K(r_1/\lambda)$ for this wavelength is 1.34 rather than the asymptotic value of 2. The 10.6-μm regressions (not shown) differ from the analytical values by an order of magnitude. There is fair agreement between the 0.53- and 1.06-μm regressions and the analytical values for $10^{-2} < W < 10^{-1}$. The differing slopes most probably result from neglecting the contributions from larger particles to the scaling laws. Whether or not particles with radii greater than 14.2 μm existed in the fog analyzed here cannot be determined. However, Junge (1952) states that r_1 for European fogs is about 20 μm and Houghton (1939) reports values exceeding 50 μm for coastal and mountain fogs in the eastern United States. Clearly, while these data demonstrate the utility of the scaling laws, additional measurements need to be made in a variety of different marine environments to include in the derived scaling laws those particles with diameters exceeding 30 μm. In addition, airborne

---

Kurnick, SW, Zitter, RN, and Williams, DB, Attenuation of infrared radiation by Fogs, Jour Opt Soc Am, 50, 578, 1960

measurements of aerosol-size distributions need be made such that scaling laws can be obtained which include horizontal and vertical variations in aerosol concentrations.

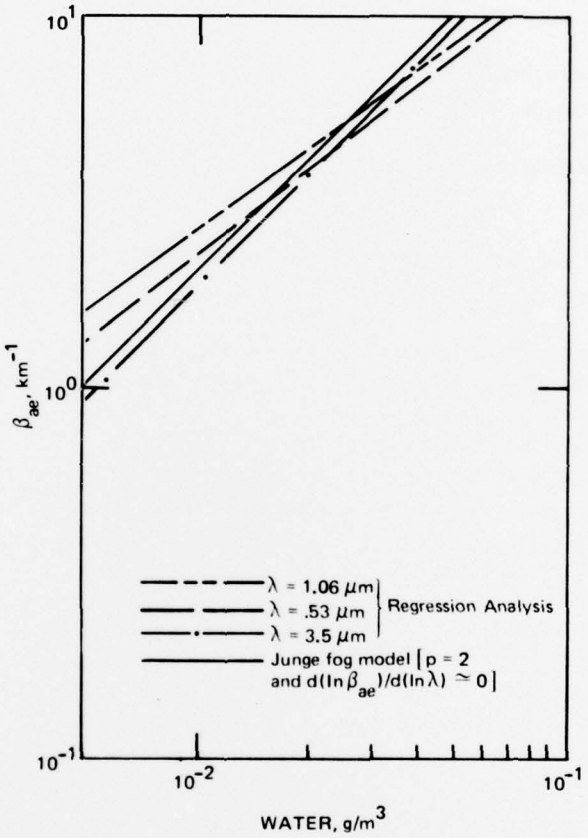

Figure 10. Comparison of extinction coefficients determined from regression analyses and those calculated by using the Junge fog drop-size distribution model.

REFERENCES

Biberman, LM, Roberts, RE, and Seekamp, LN, A comparison of electro-optical technologies for target acquisition and guidance, Institute for Defense Analysis, paper P-1218, January 1977

Deirmendjian, D, Scattering and Polarization Properties of Water Clouds and Hazes in the Visible and Infrared, Applied Optics, 3(2), 187, 1964

Eldridge, RG, Haze and fog aerosol distributions, Jour Atmos Sci, 23, 605, 1966

Houghton, HG, On the relationship between visibility and the constitution of clouds and fog, Jour Aero Sci, 6, 408, 1939

Junge, C, The size distribution and aging of natural aerosols as determined from electrical and optical data of the atmosphere, Jour Meteor, 12, 13, 1955

Kurnick, SW, Zitter, RN, and Williams, DB, Attenuation of infrared radiation by Fogs, Jour Opt Soc Am, 50, 578, 1960

Roberts, RE, Atmospheric transmission modeling: Proposed aerosol methodology with application to the Grafenwöhr atmospheric optics data base, Institute for Defense Analysis, paper P-1225, December 1976

Stone, WR, MIE and SCATCO: Programs to compute the scattering, extinction, and absorption properties of optical propagation through particle distributions, MEGATEK Corporation, San Diego, CA, Report R2005-070-F-1, 1 November 1976